

Cilostazol ameliorates atrial ionic remodeling in long-term rapid atrial pacing dogs

Zhiqiang Zhao, Weimin Li¹, Xinghua Wang, Yan Chen, Jian Li, Wansong Yang,
Lijun Cheng, Enzhao Liu, Tong Liu, Guangping Li

Department of Cardiology, Tianjin Institute of Cardiology, Second Hospital of Tianjin Medical University; Tianjin-Republic of China

¹Department of Cardiovascular Surgery, Tianjin Chest Hospital; Tianjin-Republic of China

ABSTRACT

Objective: Ionic remodeling has a close correlation with the occurrence of atrial fibrillation (AF). Atrial tachypacing remodeling is associated with characteristic ionic remodeling. The purpose of this study was to assess the efficacy of cilostazol, an oral phosphodiesterase 3 inhibitor, for preventing atrial ionic remodeling in long-term rapid atrial pacing (RAP) dogs.

Methods: We use the methods of patch-clamp and molecular biology to investigate the effect of cilostazol on ion channel and channel gene expression in long-term RAP dogs. Twenty-one dogs were randomly assigned to sham, control paced, and paced+cilostazol (5 mg/kg/d, cilo) groups, with 7 dogs in each group. The sham group was instrumented with a pacemaker but without pacing. RAP at 500 beats/min was maintained for 2 weeks in the paced and cilo groups. During the pacing, cilostazol was given orally in the cilo group. Whole-cell patch-clamp technique was used to record atrial L-type Ca^{2+} (I_{CaL}) and fast sodium channel (I_{Na}) ionic currents. Western blot and RT-PCR were applied to estimate the gene expression of the I_{CaL} α 1C (Cav1.2) and I_{Na} v1.5 α Nav1.5 α subunits. Statistical analysis was performed using SPSS 13.0.

Results: The density of I_{CaL} and I_{Na} currents (pA/pF) was significantly reduced in the paced group (I_{CaL} : -6.55 ± 1.42 vs. -4.46 ± 0.59 pA/pF; I_{Na} : -48.24 ± 10.54 vs. -30.48 ± 5.20 pA/pF, $p < 0.01$). The paced+cilo group could not increase the density of I_{CaL} currents (I_{CaL} : -4.37 ± 1.25 pA/pF, $p > 0.05$), while the I_{Na} currents were recovered (-44.54 ± 12.65 pA/pF, $p < 0.01$) compared with the paced group. The mRNA and protein expression levels of Cav1.2 and Nav1.5 α were apparently down-regulated in the paced group ($p < 0.01$), but after cilostazol treatment, both of these subunits were up-regulated significantly ($p < 0.01$).

Conclusion: Cilostazol may have protective effects on RAP-induced atrial ionic remodeling. (*Anatol J Cardiol* 2015; 15: 963-9)

Key words: atrial fibrillation, cilostazol, ionic remodeling, channel gene expression

Introduction

Atrial fibrillation (AF) is the most frequently encountered arrhythmia in the cardiology department, and no single modality is effective for all patients (1). The pathogenesis underlying AF is multi-factorial. Accumulating evidence suggests that the substrate for AF typically results from the effects of both electrical and structural remodeling. Currently available therapeutic approaches have major limitations, including limited efficacy and potentially serious side effects, such as malignant ventricular arrhythmia induction (2). An improved understanding of the mechanisms underlying AF is needed for the development of novel therapeutic approaches (3). The investigations on non-antiarrhythmic drugs have demonstrated beneficial effects in preventing the episodes of AF in both animals and human (4-6).

Atrial remodeling is the construction of the arrhythmogenic substrate of atrial AF (7). Atrial electrical remodeling is characterized by altering cellular electrical properties. The electrical activities of the heart are orchestrated by the matrix of ion channels, and ion channel remodeling involves changes in current density or in ion channel mRNA or protein expression (8).

Cilostazol is a quinolinone derivative that selectively inhibits phosphodiesterase 3 (PDE3) and has been extensively investigated as the effects of vasodilation and anti-platelet aggregation (9-13). A previous study demonstrated that cilostazol increased heart rates and improved the symptoms in patients with bradyarrhythmia, tachycardia-bradycardia syndrome, and Wenckebach-type atrioventricular block (14). Cilostazol is currently of interest to many investigators for its antiarrhythmogenic effects. Cilostazol has been investigated for anti-arrhythmic ventricular

This work was finished in Tianjin Key Laboratory of Ionic-Molecular Function of Cardiovascular Disease.

Address for Correspondence: Guangping Li, M.D., PH.D., Department of Cardiology, Tianjin Institute of Cardiology, Second Hospital of Tianjin Medical University, No. 23, Pingjiang Road, Hexi District, Tianjin City, Tianjin 300211-Republic of China
Phone: +86-22-88328368 Fax: +86-22-28261158 E-mail: gp_l@mail@sina.com

Accepted Date: 29.09.2014 **Available Online Date:** 11.11.2014

©Copyright 2015 by Turkish Society of Cardiology - Available online at www.anatoljcardiol.com
DOI:10.5152/akd.2014.5962



effects in patients with Brugada syndrome. This was assumed to be related to an increase in cytoplasmic Ca (15, 16). Similarly, PDE3 inhibition may be pro-arrhythmic in long QT syndrome (16). Whether it will be a benefit to the tachyarrhythmia has not been reported; the purpose of this study was to assess the effects of cilostazol on atrial ionic remodeling in 2-week rapid atrial pacing (RAP) dogs. The electrophysiological and cardioprotective mechanisms of cilostazol would be investigated.

Methods

Animals and materials

The animals we used in the study were approved by the Experimental Animal Administration Committee of Tianjin Medical University and Tianjin Municipal Commission for Experimental Animal Control. The approach we used was previously described to induce and maintain sustained AF in our experimental animals (17). For this study, 21 mongrel dogs of either sex, weighing between 12 and 17 kg, were randomly assigned to the sham group, paced group, or paced+cilostazol (5 mg/kg/d, cilo) group, with 7 dogs in each group. The dogs were anesthetized with intravenous pentobarbital sodium (30 mg/kg). After intubation and mechanical ventilation, under sterile technique, a modified unipolar J pacing lead (St. Jude Medical, Saint Paul, MN, USA) was inserted through the right jugular vein, and the distal end of the lead was positioned in the right atrium. Initial atrial capture was verified with the use of an external stimulator (DF5A, Suzhou, China). The proximal end of the pacing lead was then connected to a programmable pacemaker (Fudan University, Shanghai, China), which was inserted into a subcutaneous pocket in the neck. The dogs in the paced group and paced+cilo group were paced at 500 bpm (120-ms cycle length) with the use of 0.2-ms square-wave pulses at twice-threshold current for 2 weeks. The electrocardiogram (ECG) was verified after 24 h in awake dogs and then every other day to ensure continuous 1:1 atrial capture. The dogs in the sham group were instrumented without pacing and were studied 2 weeks after pacing. The dogs in the paced+cilo group received cilostazol 5 mg/kg/d by gavage for 2 weeks during pacing. Systolic blood pressure was measured by carotid artery intubation during anesthesia at baseline and after 2 weeks of RAP. ECG and blood pressure were recorded by a multi-channel physiological recorder (Hongtong, TOP2001, Shanghai, China).

Atrial cell isolation

According to the previously described cell isolation methods (18, 19), a median sternotomy was performed, and the hearts were quickly excised. After cardiac excision, the hearts were immersed in Tyrode's solution at 4°C. The solutions used for dissection and perfusion were equilibrated with 100% O₂. The left circumflex artery was cannulated and connected to the Langendorff perfusion system filled with Tyrode's solution free from CaCl₂ and saturated with 100% O₂. The heart was perfused at 25 ml/min, and the perfusion pressure was main-

tained at 80 mm Hg. The branches of the artery were ligated with silk thread to ensure adequate perfusion. The tissue was then perfused at 25 mL/min with nominally Ca²⁺-free Tyrode's solution at 37°C for 20 min, followed by a 40-min perfusion with the same solution containing collagenase (150 U/mL, CLSII, Worthington Biochemical, USA), 0.5% bovine serum albumin (Sigma Chemical Co., St. Louis, MO, USA), and 50 mM CaCl₂. Softened tissue from a well-perfused region of the LA free wall was removed with forceps, and tissue pieces were washed by Krafibruhe (KB) solution and gently triturated. Cells were dispersed by a gentle pipette for 5 min in KB solution and then filtered. After the procedure above, the myocardial cells were kept at room temperature for 60 min.

The quiescent rod-shaped cells showing clear cross-striations were chosen. A small aliquot of the solution containing the isolated cells was placed in a 1-mL chamber mounted on the stage of an inverted microscope (Olympus, Tokyo, Japan). Ten minutes was allowed for cells to adhere to the bottom of the chamber, and then the cells were superfused at 3 mL/min with Tyrode's solution (6).

Solution dispensing

Tyrode's solution contained (mmol/L) NaCl 136, KCl 5.4, MgCl₂ 0.8, CaCl₂ 1.8, NaH₂PO₄ 0.33, glucose 10, and HEPES 10, pH 7.4 (adjusted with NaOH). The KB solution contained (mmol/L) KCl 20, KH₂PO₄ 10, glucose 10, L-glutamic acid 70, taurine 10, and EGTA 10, along with 0.2% bovine serum albumin, pH 7.4 (adjusted with KOH). The pipette solution that was used to record the L-type calcium channel (*I*_{CaL}) and fast sodium channel (*I*_{Na}) contained (mmol/L) CsCl 20, MgCl₂ 1, EGTA 10, aspartic acid 80, CsOH 80, Na₃GTP 0.1, Mg₂ATP 5, HEPES 10, TEA-Cl 20, and Na₂ phosphocreatine-4H₂O 5, pH 7.25 (adjusted with CsOH). The extracellular solution recording *I*_{Na} contained (mmol/L) choline-Cl 110, NaCl 10, CsCl 20, MgCl₂ 1, CaCl₂ 1, HEPES 10, glucose 10, pH 7.4 (adjusted with NaOH). The extracellular solution recording *I*_{CaL} was the same as the Tyrode's solution.

Data acquisition

For recording ionic currents, we used the whole-cell patch-clamp technique with an Axopatch 200B amplifier (Axon Instruments). Borosilicate glass microelectrodes with a 1.5-mm outer diameter and 1.1-mm inner diameter were used, and tip resistances were kept at 2.5 to 5 MΩ. To control for cell size variability, currents were expressed as densities (pA/pF). Voltage command pulses were generated by a 12-bit digital-to-analog (D/A) converter (Digidata 1200, Axon Instruments), controlled by Clampfit 10.2 software. Recordings were sampled at 10 kHz and low-pass-filtered at 1 to 5 kHz.

Western blotting

We used the following antibodies: anti-Nav1.5a, anti-Cav1.2, and anti-GAPDH (Abcam Inc. Cambridge, UK). An equal amount of protein was loaded onto a 6% SDS denaturing polyacrylamide gel, separated by electrophoresis, transferred onto PVDF mem-

brane (Merck Millipore, USA), and incubated with the specific primary antibody overnight at 4°C. Protein levels were expressed as the ratio to levels of glyceraldehyde-3-phosphate dehydrogenase (GAPDH). The membranes were then washed and subsequently incubated with the secondary antibody conjugated to horseradish peroxidase (HRP). Protein was visualized using enhanced chemiluminescence. The resulting bands were quantified using Gene Tools software (Gene, Texas, USA).

RNA isolation and real-time RT-PCR

The LA tissue was used for molecular biological studies. Specimen were rapidly frozen in liquid nitrogen and stored separately at -80°C for further analysis. Specific oligonucleotide primer pairs for amplification of Na⁺ and Ca²⁺ channel genes were designed according to the sequences obtained from GenBank. The primers and GenBank sequence numbers specific for each channel are in Table 1. β-actin and GAPDH were included as internal controls.

A total 200 ng of total RNA underwent RT-PCR using a commercially available kit (Takara, Shiga-ken, Japan). The PCR consisted of 35 cycles of 94°C for 40 s; 51°C (Nav1.5a), 52°C (Cav1.2, β-actin), or 55°C (GAPDH) for 30 s; and 72°C for 30 s. Then, 5 μL of product was analyzed by 1% agarose gel electrophoresis.

Statistical analysis

Statistical analysis was performed using SPSS 13.0 (SPSS Inc., Chicago, IL, USA) and GraphPad Prism 5.0 software (GraphPad Software, Inc., California, USA). Continuous vari-

Table 1. Primers for RT-PCR

Gene	Sequence numbers	Primer (5'→3')	Size (BP)
Nav1.5α	NM_001002994	F: TGAATGTCCTCCTCGTCTG	424
		R: TGTTGGTTGAAGTTGTCG	
Cav1.2	AB262537.1	F: CCCTGCTGTGGACCTTCA	288
		R: CACCTTCCGTGCTGTTGC	
β-actin	AF021873.2	F: CAGAGCAAGCGGGGCATC	392
		R: AGGTAGTCAGTCAGGTCC	
GAPDH	NM001003142.1	F: ACCACAGTCCATGCCATCAC	261
		R: CACCACCTTCTTGATGTCATC	

Table 2. Hemodynamic parameters before and after pacing in each group

Group	Heart rate, bpm			Systolic blood pressure, mm Hg		
	Before pacing	Paced for 2 weeks	P	Before pacing	Paced for 2 weeks	P
Sham	197±12	199±16	>0.05	136.4±7.5	134.6±7.8	>0.05
Paced	198±9	198±13	>0.05	138.3±10.1	132.4±7.5	>0.05
Cilo	196±14	198±15	>0.05	136.2±7.8	135.8±6.8	>0.05
F	0.185	0.029		0.122	0.389	
P	>0.05	>0.05		>0.05	>0.05	

Data are presented as mean±SD; *Bonferroni t-test

ables are expressed as mean±SD. Kolmogorov-Smirnov test was used to test the distribution of numeric variables, and statistical comparisons among groups with normal distribution were performed by one-way analysis of variance (ANOVA). If significant effects were indicated by ANOVA, a *t*-test with Bonferroni correction or Dunnett's test was used to evaluate the significance of differences between individual mean values. A two-tailed *p*<0.05 was considered significant.

Results

Hemodynamic parameters

As shown in Table 2, there was no significant difference in ventricular rate or systolic blood pressure between groups at baseline (*p*>0.05), and no difference was found during the pacing (*p*>0.05); the blood pressure and heart rate were not changed by rapid atrial pacing in each group after 2 weeks (*p*>0.05). All animals kept a good appetite and physiological conditions.

I_{CaL} changes and gene expression

In the present study, any contaminating effects of I_{CaL} run-down were minimized by beginning all studies 5 min after membrane rupture. Depolarizing 200-millisecond pulses from -40 mV to voltages ranging from -50 mV to +50 mV elicited typical I_{CaL}. Figure 1A shows the I-V curves of I_{CaL} obtained from the dogs of each group. Figure 1B shows the mean±SEM of peak I_{CaL} current densities; RAP was associated with a decrease in I_{CaL} density. I_{CaL} density was reduced significantly by RAP. Maximum peak I_{CaL} density averaged to -4.46±0.59 pA/pF in the paced group (n=10 cells) compared with -6.55±1.42 pA/pF in sham dogs (n=9 cells) (*p*<0.01). After 2 weeks of RAP, cilostazol (5 mg/kg/d, cilo) (-4.37±1.25 pA/pF, n=8 cells) did not change the maximum peak density of I_{CaL} compared with the paced group (*p*>0.05). The protein levels of Cav1.2 decreased in the paced group compared with the sham group (Cav1.2: paced group 0.31±0.03 vs. sham group 1.0, *p*<0.01).

Figure 1C shows a representative gel obtained by semi-quantitative RT-PCR for Cav1.2. Figure 1D shows the mean±SEM Cav1.2 mRNA concentration in hearts (1 independent determination per heart) from each group of dogs. Data are presented as relative gene expression (n=6). The mRNA levels of Cav1.2

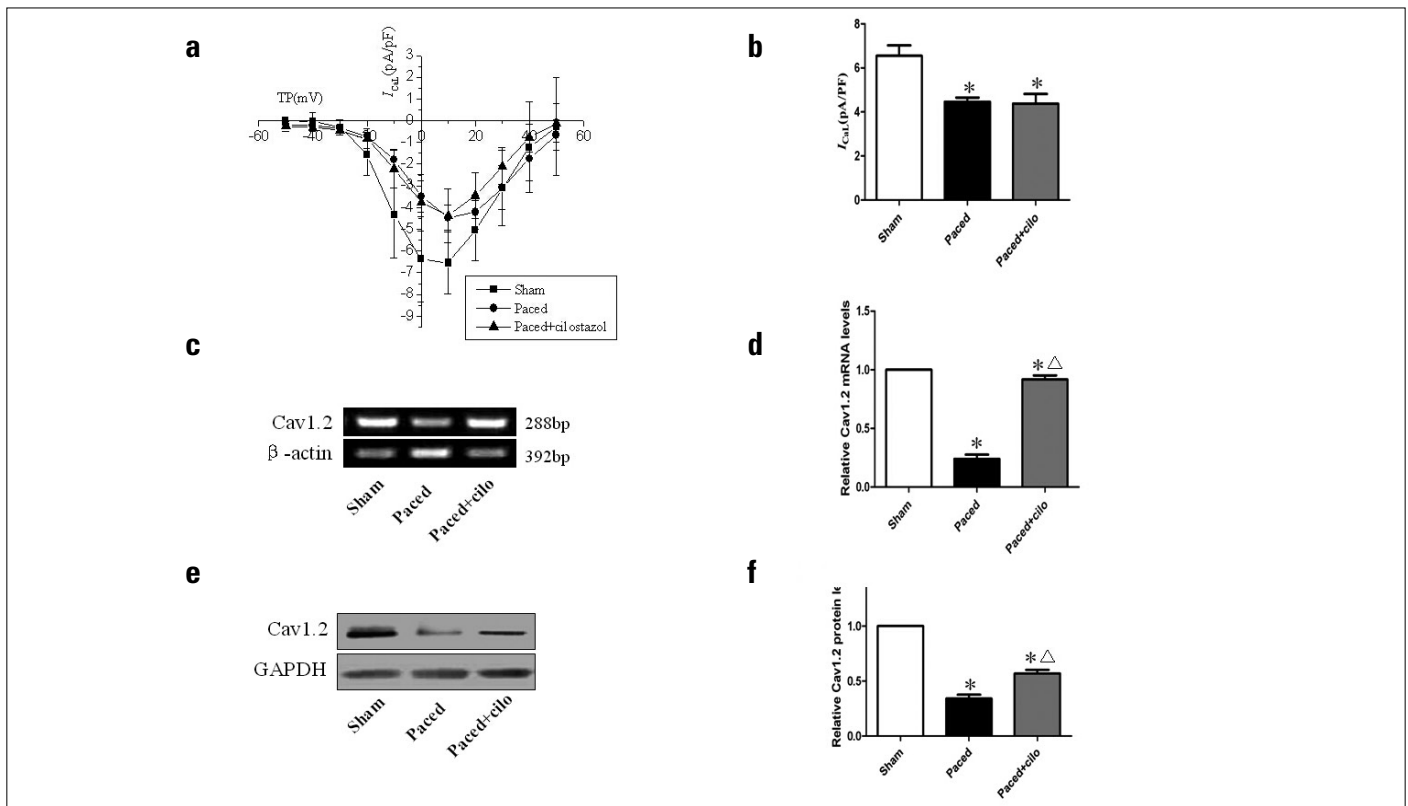


Figure 1. a-f. I-V curves of I_{CaL} and the relative gene expression levels of Cav1.2 in three groups. (a) I-V curves of I_{CaL} obtained from dogs of various groups. TP (test potential). (b) Columns and error bars indicate mean \pm SEM, respectively. (c) Representative Cav1.2 RT-PCR results. (d) Columns and error bars indicate mean \pm SEM of Cav1.2 RT-PCR results. (e) Representative Cav1.2 western blot results. (f) Columns and error bars indicate mean \pm SEM Cav1.2 western blot results. The relative gene expression levels of Cav1.2 were decreased by RAP. Cilostazol markedly upregulated the gene expression levels of Cav1.2. Data are presented as relative gene expression (n=6). * P <0.01 vs. corresponding value in sham group; Δ P <0.01 vs. corresponding value in paced group

decreased in the paced group compared with the sham group (p <0.01). The paced+cilo group increased the mRNA levels of Cav1.2 compared with the paced group (p <0.01). Figure 1E shows representative western blots of Cav1.2. The 288-kDa immunoreactive band. Figure 1F illustrates quantitative Cav1.2 immunoreactivity of the western blot hybridization. Data are presented as relative gene expression (n=6). GAPDH was used as a loading control. The protein levels of Cav1.2 were upregulated in the paced+cilo group (p <0.01).

I_{Na} changes and gene expression

The I-V curves relation for I_{Na} in each group are revealed in Figure 2A; peak I_{Na} density was shown as a function of test potential (TP). Any contaminating effects of I_{Na} rundown were also minimized by beginning all studies 5 min after membrane rupture. Depolarizing 200-millisecond pulses from -90 mV to voltages ranging from -80 mV to +60 mV elicited a typical I_{Na} . Figure 2B illustrates that RAP was associated with a decrease in I_{Na} density. I_{Na} density was reduced highly significantly by RAP. Maximum peak I_{Na} density averaged to -30.48 ± 5.20 pA/pF in the paced group (n=6 cells) compared with -48.24 ± 10.54 pA/pF in sham dogs (n=10 cells) (p <0.05). After 2 weeks of RAP, in the cilostazol group (-44.54 ± 12.65 pA/pF, n=9 cells), the density of I_{Na} (-58.62 ± 16.17 pA/pF, n=8

cells) was significantly higher than that in the paced group and sham group (p <0.01).

The mRNA levels of Nav1.5 α were also evaluated. Figure 2C shows a gel obtained by semiquantitative RT-PCR for the Nav1.5 α subunit. The left band in each lane corresponds to the Nav1.5 α mRNA product, and the right band is the internal standard. Figure 2D shows the mean \pm SEM Nav1.5 α mRNA concentration in hearts (1 independent determination per heart) from each group of dogs. Data are presented as relative gene expression (n=6). The mRNA levels of Nav1.5 α decreased in the paced group compared with the sham group (p <0.01). The paced+cilo group increased the mRNA levels of Nav1.5 α compared with the paced group (p <0.01). The protein expression of Nav1.5 α was down-regulated by RAP. Cilostazol could induce the up-regulation of protein expression of Nav1.5 α (Fig. 2E, 2F).

Discussion

The major finding of this study is that cilostazol may have beneficial effects on atrial ionic remodeling in long-term RAP dogs.

Atrial electrophysiology change is one of the main characteristics of AF, which is called electrical remodeling. Wijffels et al. (7) reported that atrial electrical remodeling played a key role

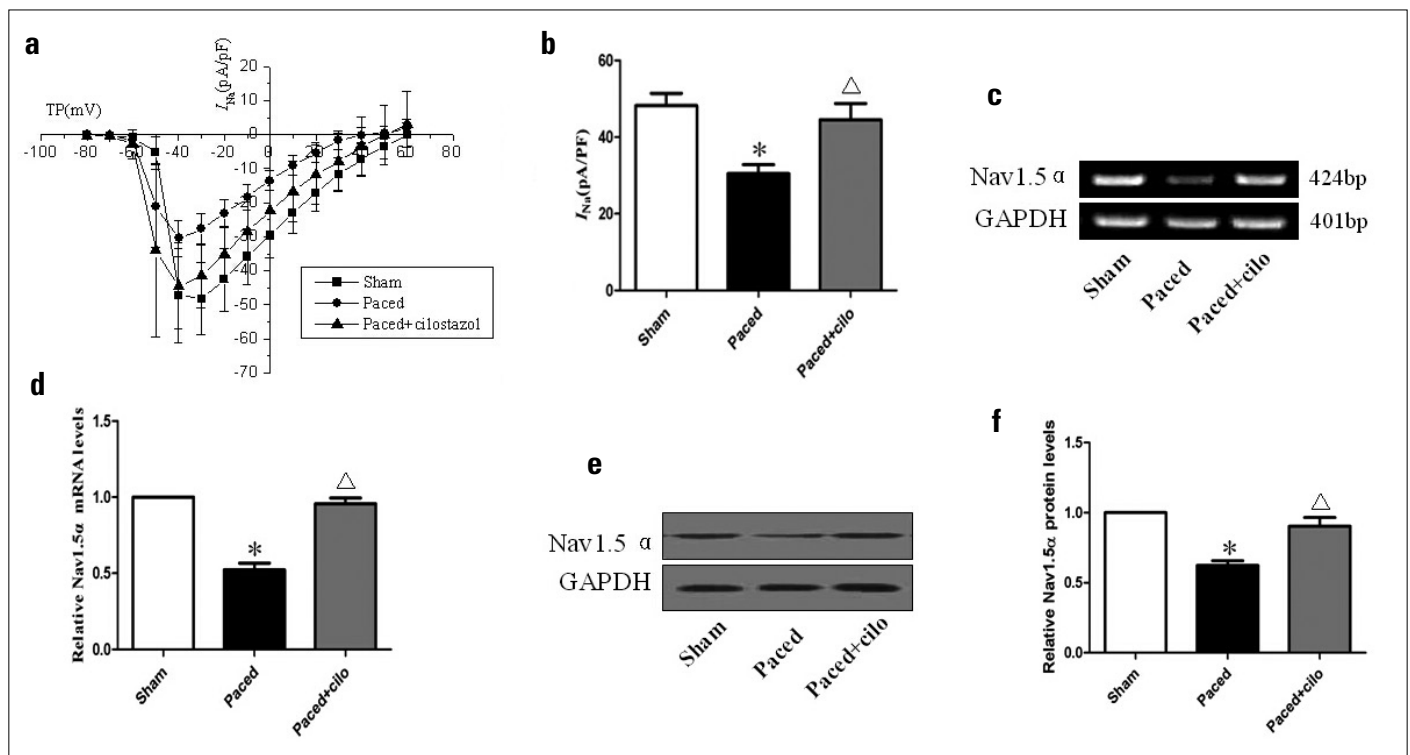


Figure 2. a-f. I-V curves of I_{Na} and the relative gene expression levels of Nav1.5 α in the three groups. (a) I-V curves of I_{Na} obtained from dogs of various groups. TP (test potential). (b) Columns and error bars indicate mean \pm SEM, respectively. (c) Representative the Nav1.5 α RT-PCR results. (d) Columns and error bars indicate mean \pm SEM. (e) Representative Nav1.5 α western blot results. (f) Columns and error bars indicate mean \pm SEM Nav1.5 α western blot results. The relative gene expression levels of Nav1.5 α were decreased by RAP. Cilostazol markedly upregulated the gene expression levels of Nav1.5 α . Data are presented as relative gene expression (n=6). * P <0.01 vs. corresponding value in sham group, Δ P <0.01 vs. corresponding value in paced group

in the development, maintenance, and recurrence of AF. Research (20-22) has shown that the changes in reduced ion current density, including I_{CaL} , I_{Na} , etc., are an important basis for early electrical remodeling in AF and result in a functional substrate that supports the maintenance of AF.

In the experiment, we used the AOO model of a buried implanted pacemaker, with the right external jugular vein approach. The incision was small, had a low rate of infection, avoided the operation method of thoracotomy, and improved the operation efficiency and success rate. During the experiment, we used the method of monitoring the limb lead ECG to detect the effectiveness of high-speed continuous atrial pacing and evaluate the successful rate of the model. After 2 weeks, a median sternotomy was performed; we checked the location of the electrode at the same time, and the hearts were quickly excised, and next, the electrophysiological experiments were performed. The electrode position on the right atrial and right or appendage was regarded as a successful model. The application of the model was safe and reliable, and the AF-induced rate was more than 80%. In the present study, the ventricular rate was not controlled by atrioventricular (AV) node block, and it was a pity that we did not assess ventricular function with echocardiography. But, we found that the ventricular rate and blood pressure were not significantly changed by RAP in each group. Thus, the ventricular tachycardia-induced left ventricular dysfunction might not have been caused by the pacing or might not

have contributed to the development of atrial remodeling in the RAP dog model.

Yue et al. (18) showed that L-type calcium channel (I_{CaL}) plays a significant role in maintaining the plateau in canine atrial myocytes. Grunnet et al. (23) indicated that I_{CaL} plays a crucial part in the regulation of human atrial frequency-dependent action potential duration (APD) and endocardial return percentage (ERP). Nav1.5 is the principal Na^+ channel isoform expressed in cardiomyocytes. Nav1.5 has also been observed in the endoplasmic reticulum of dog myocytes (24). Abriel et al. (25) reported that Nav1.5 associates with partner proteins, which may be adaptor proteins, enzymes which interact with and modify the channel, and proteins modulating the biophysical properties of Nav1.5 upon binding. Nav1.5 is essential for the conduction of electrical impulse and has a close correlation with AF (26-28). Lu et al. (29) indicated that RAP could induce acute stages of atrial electrical remodeling. Atrial tachycardia is a sufficient stimulus to induce the changes typical of AF-induced remodeling (17).

The major finding of this study is that cilostazol may have beneficial effects on atrial ionic remodeling in long-term RAP dogs. Our data indicate that the I_{CaL} current was not changed in the cilostazol-treated group but increased Cav1.2 gene expression in our animal model of RAP. The reasons for the increase of Cav1.2 gene expression found in the paced+cilostazol group in our study are not apparent and deserve further investigation.

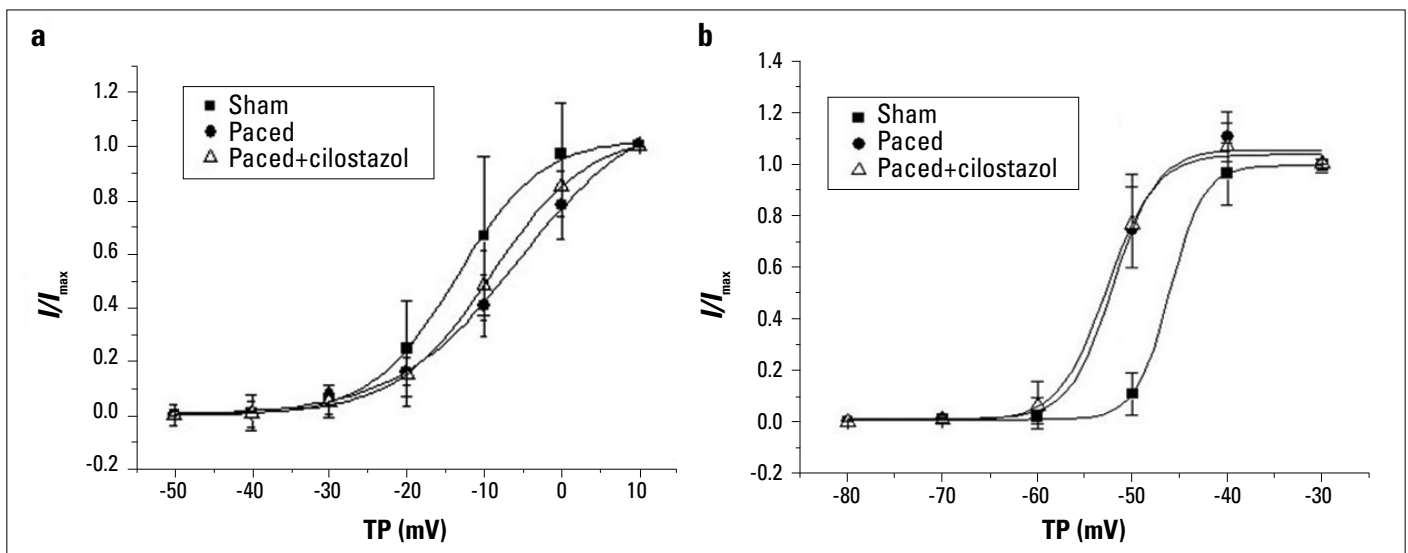


Figure 3. a, b. Active curves of I_{CaL} and I_{Na} in the three groups. (a) Active curves of I_{CaL} obtained from dogs of various groups. TP (test potential). (b) Active curves of I_{Na} obtained from dogs of various groups

The I-V curve indicates that I_{CaL} was not changed in the cilostazol-treated group. As a result, we investigated the active curve of I_{CaL} and found that there were significant differences in the sham group and paced+cilo group in the curve; although the entire current range had no significant change, cilostazol still restored the active status of I_{CaL} (Fig. 3A) probably because the drug dose and treatment time were not enough.

The present study showed that cilostazol could up-regulate I_{Na} current and its channel gene expression in the paced+cilostazol group compared to in paced group. The human cardiac Na^+ channel, voltage-gated $Nav1.5\alpha$ (encoded by the *SCN5A* gene), is responsible for the fast depolarization upstroke of the cardiac action potential and serves as a molecular target for developing antiarrhythmic drugs (30, 31). The mutations in *SCN5A* may predispose patients with or without underlying heart diseases to AF, expanding the clinical spectrum of disorders of the cardiac Na^+ channel to AF (31, 32). Cilostazol could up-regulate I_{Na} current in the paced+cilostazol group compared to the paced group. However, there were no obvious changes of the I_{Na} active curve between the paced and paced+cilo groups (Fig. 3B). These results indicated that cilostazol may have the function to restore the I_{Na} current by not affecting its active status and might act by other ways to regulate the current.

Increased evidence has demonstrated that cilostazol could have many potential benefits on the heart, and cilostazol may have dual inhibitory effects in the heart (33). Cilostazol has presented different effects from other PDE3 inhibitors, especially adenosine uptake inhibition. Therefore, cilostazol may serve as an effective cardioprotective drug, with its beneficial effects in preventing arrhythmia. Investigations on the effects of cilostazol on heart rate variability (HRV) have shown that cilostazol significantly improves a slow heart rate (34, 35). However, it is important to note that the evidence regarding cilostazol and tachyarrhythmia is still limited and unclear. Currently, as we know, there are fewer studies that directly have investigated the effect of cilostazol in AF. In a recent study, Alizade et al. (36) indicated

that cilostazol could decrease total atrial conduction time duration in patients with peripheral artery disease, which may also prevent the development and/or recurrence of AF.

Study limitations

In the present study, we did not assess the overall electrophysiological inter-atrial conduction time (IACT), atrial effective refractory period (AERP), and vulnerability to AF. We also did not evaluate the cardiac function with echocardiography. We also did not evaluate other ion currents in our study. These limitations should be solved in future studies with different designs.

Conclusion

This study, for the first time, demonstrated that in the atrial tissue of chronic rapid atrial pacing dogs, cilostazol 5 mg/kg/d could effectively suppress the down-regulation of I_{Na} currents and up-regulation of *Cav1.2* and *Nav1.5a* gene expression. In conclusion, we found for the first time that cilostazol ameliorated atrial ionic remodeling in a canine model of RAP. Our study provides further evidence for the role of cilostazol in regulating tachyarrhythmia. Cilostazol 5 mg/kg/d did not affect the current densities of I_{CaL} in paced dogs. Cilostazol may prevent atrial ionic remodeling and may serve as a novel therapeutic approach to the prevention of AF.

Conflict of interest: None declared.

Peer-review: Externally peer-reviewed.

Authorship contributions: Concept - G.L.; Design - G.L., T.L., E.L.; Supervision - Z.Z., L.C.; Resource - G.L.; Materials - J.L., X.W., W.Y.; Data collection &/or processing - Z.Z., W.L., L.C.; Analysis &/or interpretation - Y.C., L.C., W.L., X.W.; Literature search - T.L., E.L., X.W., J.L.; Writing - Z.Z.; Critical review - T.L., E.L., W.Y., W.L., Y.C.; Other - W.L., Z.Z., W.Y., J.L., Y.C.

References

- Camm AJ, Kirchhof P, Lip GY, Schotten U, Savelieva I, Ernst S, et al. Guidelines for management of atrial fibrillation: the Task Force for the Management of Atrial Fibrillation of the European Society of Cardiology (ESC). *Eur Heart J* 2010; 31: 2369-429. [\[CrossRef\]](#)
- Dobrev D, Nattel S. New antiarrhythmic drugs for treatment of atrial fibrillation. *Lancet* 2010; 375: 1212-23. [\[CrossRef\]](#)
- Nattel S. From guidelines to bench: implications of unresolved clinical issues for basic investigations of atrial fibrillation mechanisms. *Can J Cardiol* 2011; 27: 19-26. [\[CrossRef\]](#)
- Moro C, Hernández-Madrid A, Matía R. Non-antiarrhythmic drugs to prevent atrial fibrillation. *Am J Cardiovasc Drugs* 2010; 10: 165-73. [\[CrossRef\]](#)
- Savelieva I, Kakouros N, Kourliouros A, Camm AJ. Upstream therapies for management of atrial fibrillation: review of clinical evidence and implications for European Society of Cardiology guidelines. Part I: primary prevention. *Europace* 2011; 13: 308-28. [\[CrossRef\]](#)
- Liu E, Xu Z, Li J, Yang S, Yang W, Li G. Enalapril, irbesartan, and angiotensin-(1-7) prevent atrial tachycardia-induced ionic remodeling. *Int J Cardiol* 2011; 146: 364-70. [\[CrossRef\]](#)
- Wijffels MC, Kirchhof CJ, Dorland R, Allesie MA. Atrial fibrillation begets atrial fibrillation. A study in awake chronically instrumented goats. *Circulation* 1995; 92: 1954-68. [\[CrossRef\]](#)
- Brundel BJ, Van Gelder IC, Henning RH, Tieleman RG, Tuinenburg AE, Wietes M, et al. Ion channel remodeling is related to intraoperative atrial effective refractory periods in patients with paroxysmal and persistent atrial fibrillation. *Circulation* 2001; 103: 684-90. [\[CrossRef\]](#)
- Kanlop N, Chattipakorn S, Chattipakorn N. Effects of cilostazol in the heart. *J Cardiovasc Med (Hagerstown)* 2011; 12: 88-95. [\[CrossRef\]](#)
- Han SW, Lee SS, Kim SH, Lee JH, Kim GS, Kim OJ, et al. Effect of Cilostazol in acute Lacunar Infarction based on Pulsatility index of transcranial Doppler (ECLIPSe): a multicenter, randomized, double-blind, placebo-controlled trial. *Eur Neurol* 2013; 69: 33-40. [\[CrossRef\]](#)
- Kambayashi J, Liu Y, Sun B, Shakur Y, Yoshitake M, Czerwicz F. Cilostazol as a unique antithrombotic agent. *Curr Pharm Des* 2003; 9: 2289-302. [\[CrossRef\]](#)
- Kim MJ, Park KG, Lee KM, Kim HS, Kim SY, Kim CS, et al. Cilostazol inhibits vascular smooth muscle cell growth by down regulation of the transcription factor E2F. *Hypertension* 2005; 45: 552-6. [\[CrossRef\]](#)
- Watanabe K, Ikeda S, Komatsu J, Inaba S, Suzuki J, Sueda S, et al. Effect of cilostazol on vasomotor reactivity in patients with vasospastic angina pectoris. *Am J Cardiol* 2003; 92: 21-5. [\[CrossRef\]](#)
- Atarashi H, Endoh Y, Saitoh H, Kishida H, Hayakawa H. Chronotropic effects of cilostazol, a new antithrombotic agent, in patients with bradyarrhythmias. *J Cardiovasc Pharmacol* 1998; 31: 534-9. [\[CrossRef\]](#)
- Tsuchiya T, Ashikaga K, Honda T, Arita M. Prevention of ventricular fibrillation by cilostazol, an oral phosphodiesterase inhibitor, in a patient with Brugada syndrome. *J Cardiovasc Electrophysiol* 2002; 13: 698-701. [\[CrossRef\]](#)
- Shimizu W, Aiba T, Antzelevitch C. Specific therapy based on the genotype and cellular mechanism in inherited cardiac arrhythmias. Long QT syndrome and Brugada syndrome. *Curr Pharm Des* 2005; 11: 1561-72. [\[CrossRef\]](#)
- Nattel S, Li D. Ionic remodeling in the heart: pathophysiological significance and new therapeutic opportunities for atrial fibrillation. *Circ Res* 2000; 87: 440-7. [\[CrossRef\]](#)
- Yue L, Feng J, Li GR, Nattel S. Transient outward and delayed rectifier currents in canine atrium: properties and role of isolation methods. *Am J Physiol* 1996; 270: H2157-68.
- Li D, Melnyk P, Feng J, Wang Z, Petrecca K, Shrier A, et al. Effects of experimental heart failure on atrial cellular and ionic electrophysiology. *Circulation* 2000; 101: 2631-8. [\[CrossRef\]](#)
- Yue L, Melnyk P, Gaspo R, Wang Z, Nattel S. Molecular mechanisms underlying ionic remodeling in a dog model of atrial fibrillation. *Circ Res* 1999; 84: 776-84. [\[CrossRef\]](#)
- Nattel S, Dobrev D. The multi-dimensional role of calcium in atrial fibrillation pathophysiology: mechanistic insights and therapeutic opportunities. *Eur Heart J* 2012; 33: 1870-7. [\[CrossRef\]](#)
- Heijman J, Dobrev D. Systems approaches to post-operative atrial fibrillation-do they help us to better understand the ionic basis of the arrhythmogenic substrate? *J Mol Cell Cardiol* 2012; 53: 320-2. [\[CrossRef\]](#)
- Grunnet M, Bentzen BH, Sørensen US, Diness JG. Cardiac ion channels and mechanisms for protection against atrial fibrillation. *Rev Physiol Biochem Pharmacol* 2012; 162: 1-58.
- Zimmer T, Biskup C, Dugarmaa S, Vogel F, Steinbis M, Böhle T, et al. Functional expression of GFP-linked human heart sodium channel (hH1) and subcellular localization of the a subunit in HEK293 cells and dog cardiac myocytes. *J Membr Biol* 2002; 186: 1-12. [\[CrossRef\]](#)
- Abriel H, Kass RS. Regulation of the voltage-gated cardiac sodium channel Nav1.5 by interacting proteins. *Trends Cardiovasc Med* 2005; 15: 35-40. [\[CrossRef\]](#)
- Nerbonne JM, Kass RS. Molecular physiology of cardiac repolarization. *Physiol Rev* 2005; 85: 1205-53. [\[CrossRef\]](#)
- Laitinen-Forsblom PJ, Makynen P, Makynen H, Yli-Mäyry S, Virtanen V, Kontula K, et al. SCN5A mutation associated with cardiac conduction defect and atrial arrhythmias. *J Cardiovasc Electrophysiol* 2006; 17: 480-5. [\[CrossRef\]](#)
- Chen LY, Ballew JD, Herron KJ, Rodeheffer RJ, Olson TM. A common polymorphism in SCN5A is associated with lone atrial fibrillation. *Clin Pharmacol Ther* 2007; 81: 35-41. [\[CrossRef\]](#)
- Lu Z, Scherlag BJ, Lin J, Niu G, Fung KM, Zhao L, et al. Atrial fibrillation begets atrial fibrillation: autonomic mechanism for atrial electrical remodeling induced by short-term rapid atrial pacing. *Circ Arrhythm Electrophysiol* 2008; 1: 184-92. [\[CrossRef\]](#)
- Gellens ME, George AL Jr, Chen LQ, Chahine M, Horn R, Barchi RL, et al. Primary structure and functional expression of the human cardiac tetrodotoxin-insensitive voltage-dependent sodium channel. *Proc Natl Acad Sci USA* 1992; 89: 554-8. [\[CrossRef\]](#)
- Darbar D, Kannankeril PJ, Donahue BS, Kucera G, Stubblefield T, Haines JL, et al. Cardiac sodium channel (SCN5A) variants associated with atrial fibrillation. *Circulation* 2008; 117: 1927-35. [\[CrossRef\]](#)
- Chen L, Zhang W, Fang C, Jiang S, Shu C, Cheng H, et al. Polymorphism H558R in the human cardiac sodium channel SCN5A gene is associated with atrial fibrillation. *J Int Med Res* 2011; 39: 1908-16. [\[CrossRef\]](#)
- Liu Y, Shakur Y, Yoshitake M, Kambayashi Ji J. Cilostazol (pletal): a dual inhibitor of cyclic nucleotide phosphodiesterase type 3 and adenosine uptake. *Cardiovasc Drug Rev* 2001; 19: 369-86. [\[CrossRef\]](#)
- Toyonaga S, Nakatsu T, Murakami T, Kusachi S, Mashima K, Tominaga Y, et al. Effects of cilostazol on heart rate and its variation in patients with atrial fibrillation associated with bradycardia. *J Cardiovasc Pharmacol Ther* 2000; 5: 183-91. [\[CrossRef\]](#)
- Moriya I, Takahashi T, Nomura Y, Kawaura K, Kusaka K, Yamakawa J, et al. Chronotropic effect of the antithrombotic agent cilostazol in a patient with sick sinus syndrome and syncope. *J Int Med Res* 2004; 32: 549-51. [\[CrossRef\]](#)
- Alizade E, Şahin M, Şimsek Z, Açar G, Bulut M, Güler A, et al. Cilostazol decreases total atrial conduction time in patients with peripheral artery disease. *Perfusion* 2014; 29: 265-71. [\[CrossRef\]](#)